OXFORD

JNCI J Natl Cancer Inst, (2015) 107(4): dju505

doi:10.1093/jnci/dju505
First published online February 7, 2015
Article

ARTICLE

Role of MYC-Regulated Long Noncoding RNAs in Cell Cycle Regulation and Tumorigenesis

Taewan Kim*, Young-Jun Jeon*, Ri Cui, Ji-Hoon Lee, Yong Peng, Sung-Hak Kim, Esmerina Tili, Hansjuerg Alder, Carlo M. Croce

Affiliations of authors: Department of Molecular and Cellular Oncology, The University of Texas MD Anderson Cancer Center, Houston, TX (TK); Department of Molecular Virology, Immunology and Medical Genetics (TK, YJJ, RC, ET, HA, CMC), Department of Neurological Surgery (SHK), and Department of Anesthesiology (ET), Wexner Medical Center, The Ohio State University, OH; School of Biological Sciences, Seoul National University and National Creative Research Initiative Center for Symbiosystem, Seoul, Republic of Korea (JHL); State Key Laboratory of Biotherapy/Collaborative Innovation Center of Biotherapy, West China Hospital, Sichuan University, Chengdu, China (YP); School of Life Sciences and Biotechnology, Korea University, Republic of Korea (SHK).

*Authors contributed equally to this work.

Correspondence to: Carlo M. Croce, MD, 1082 BRT, 460 West 12th Ave, Columbus, OH 43210 (e-mail: carlo.croce@osumc.edu).

Abstract

Background: The functions of long noncoding RNAs (lncRNAs) have been identified in several cancers, but the roles of lncRNAs in colorectal cancer (CRC) are less well understood. The transcription factor *MYC* is known to regulate lncRNAs and has been implicated in cancer cell proliferation and tumorigenesis.

Methods: CRC cells and tissues were profiled to identify lncRNAs differentially expressed in CRC, from which we further selected MYC-regulated lncRNAs. We used luciferase promoter assay, ChIP, RNA pull-down assay, deletion mapping assay, LC-MS/MS and RNA immunoprecipitation to determine the mechanisms of MYC regulation of lncRNAs. Moreover, soft agar assay and in vivo xenograft experiments (four athymic nude mice per group) provided evidence of MYC-regulated lncRNAs in cancer cell transformation and tumorigenesis. The Kaplan-Meier method was used for survival analyses. All statistical tests were two-sided.

Results: We identified lncRNAs differentially expressed in CRC ($P < .05$, greater than two-fold) and verified four lncRNAs upregulated and two downregulated in CRC cells and tissues. We further identified MYC-regulated lncRNAs, named *MYCLo*s. The MYC-regulated *MYCLo*s may function in cell proliferation and cell cycle by regulating MYC target genes such as *CDKN1A* (p21) and *CDKN2B* (p15), suggesting new regulatory mechanisms of MYC-repressed target genes through lncRNAs. RNA binding proteins including HuR and hnRNPK are involved in the function of *MYCLo*s by interacting with *MYCLo-1* and *MYCLo-2*, respectively. Knockdown experiments also showed that *MYCLo-2*, differentially expressed not only in CRC but also in prostate cancer, has a role in cancer transformation and tumorigenesis.

Conclusions: Our results provide novel regulatory mechanisms in MYC function through lncRNAs and new potential lncRNA targets of CRC.

Mammalian genomes encode a large number of noncoding RNAs from small regulatory RNAs such as microRNAs and Piwi-associated RNAs (piRNAs) to long noncoding RNAs (lncRNAs; longer than 200 bp) (1,2). To date, more than 30 000 long noncoding RNAs (lncRNAs) have been annotated or identified (3–6). A few lncRNAs such as *CCAT1* (*CARLo-5*) and *CCAT2* have been

Received: May 12, 2014; **Revised:** August 8, 2014; **Accepted:** December 19, 2014

also reported in colorectal cancer (CRC) (7–9). However, an enormous number of lncRNAs still remain to be elucidated and characterized.

The proto-oncogene *MYC* is frequently amplified in many types of cancer, including CRC (10,11). The gene product of *MYC* is a transcription factor that regulates transcription of many protein-coding genes and noncoding RNAs such as microRNAs, and the downstream genes are involved in various cellular processes including cell cycle, differentiation, cell growth, metabolism, cell adhesion, angiogenesis, chromosome instability, and cell transformation (10). To date, a large number of MYC-regulated genes including *CDKN2B* (p15) and *CDKN1A* (p21) have been identified (10,12–14). Those target genes such as *CDKN1A* and *CDKN2B* are critical intermediators of MYC-mediated tumorigenesis (13,15).

Methods

LncRNA Microarray

Total RNA extracted from four normal colon-derived fibroblast cell lines (CCD-18Co, CCD-33Co, CCD-112CoN, CCD-841CoN), four colorectal cancer cell lines (HT29, SW620, HCT116, RKO), three primary CRC tissue samples and their matched normal adjacent tissues (NATs) (Origene), HCT116 cells treated with siCTRL or siMYC and RKO cells treated with siCTRL or siMYC that was subjected to lncRNA microarray. Further details are available in Supplementary Methods (available online).

Patients and Primary Colorectal and Prostate Tissue Samples

Primary colorectal and prostate tissue samples were provided by the Department of Pathology at The Ohio State University (OSU). All human tissues were obtained according to a protocol approved by the Ohio State Institutional Review Board. Tissue samples were fresh-frozen in liquid nitrogen after surgery and kept at -80°C. Frozen tissue samples were homogenized using the Tissue Ruptor (QIAGEN) before RNA extraction. Total RNA was extracted using Trizol (Invitrogen) in accordance with manufacturer's instructions.

Xenograft and Tumor-Free Survival Analysis

Animal experiments were approved by The Ohio State University animal care and use committee and conducted following The Ohio State University animal policy in accordance with National Institutes of Health guidelines. 0.5 million cells transfected with indicated siRNAs 24 hours before injection were subcutaneously injected into the right flanks of five-week-old female athymic nude mice (Jackson laboratory, four mice per group). Further details are available in Supplementary Methods (available online).

NanoString Gene Expression Assay and Data Analysis

For NanoString Gene expression assay analyses, the nCounter Virtual Cell Cycle Gene Set was used, following manufacturer's instructions (NanoString Technologies). Briefly, total RNA (100 ng) was used as input for nCounter mRNA sample preparation reactions. All sample preparation was performed according to manufacturer's instructions (NanoString Technologies). Further details are available in Supplementary Methods (available online).

Rapid Amplification of cDNA Ends (RACE)

5' and 3' RACE were performed using the SMARTer RACE cDNA Amplification Kit (Clontech). All procedures were done in accordance with manufacturer's instruction. Total RNA from HT29 or SW620 was used. Polymerase chain reaction (PCR) of the internal region was performed when starting points of 5' and 3' RACE had an unamplified gap. All primers used for RACE are presented in Supplementary Table 5 (available online).

Cells, Oligonucleotides, and Transfection

All cell lines were purchased from American Type Culture Collection (ATCC) and cultured as recommended by the ATCC. All experiments with cells were done between passage 4–9. All custom siRNAs were designed by the Dharmacon custom siRNA design tool based on sequence information identified by RACE. For each MYCLo, two kinds of custom siRNAs were designed and used. Further details are available in the Supplementary Methods (available online).

Quantitative Real-Time PCR

Total RNA was prepared from cells using TRIZOL (Invitrogen) in accordance with manufacturer's instructions. Total RNA was subjected to quantitative real-time PCR (qRT-PCR). RNA levels were analyzed using TaqMan Gene Expression Assays, in accordance with manufacturer's instructions (Applied Biosystems). All RT reactions, including no-template controls and RT minus controls, were run in a GeneAmp PCR 9700 Thermocycler (Applied Biosystems). Further details are available in the Supplementary Methods (available online).

Cell Proliferation Assay

For cell proliferation assay, the MTS assay from Promega (CellTiter 96 AQueous One Solution Cell Proliferation Assay) was used following manufacturer's instruction. Briefly, cells in a 96-wells plate were incubated for 72 hours or 96 hours in a humidified 5% CO_2 atmosphere after transfection with indicated siRNAs, followed by addition of 20 µL CellTiter 96 AQueous One Solution and one- to four-hour incubation in humidified 5% CO_2 atmosphere. The absorbance at 490 nm was recorded.

Flow Cytometry Analysis

For DNA content analysis, cells were fixed in methanol at -20° C, washed again, rehydrated, resuspended in phosphate-buffered saline containing 2 µg/mL propidium iodide (PI), and 5 µg/mL RNase A and analyzed by BD FACS Calibur Flow Cytometer.

Luciferase Reporter Assay

Cells were plated in 24-well plates 24 hours before transfection. All plasmids constructed with pGL4-luc2P vectors were cotransfected with control Renilla luciferase plasmid (pGL4-hRluc/TK) and siRNAs, as indicated by using Lipofectamine 2000

(Invitrogen). Further details are available in the Supplementary Methods (available online).

Soft Agar Colony Formation Assay

Soft agar colony formation assay was performed with the CytoSelect cell transformation assay (Cell Biolab, Inc.) in accordance with the manufacturer's instructions. The cells transfected with indicated siRNA were incubated for 24 hours, followed by a soft agar colony formation assay.

RNA Pull-Down Assay, Deletion Mapping, RIP, ChIP, and Antibodies

RNA pull-down and deletion mapping were performed using a Magnetic RNA-Protein Pull-Down kit (Pierce) in accordance with the manufacturer's instructions. The full-length or deleted RNA samples were prepared using the LITMUS28i system and T7 in vitro transcription kit (NEB) followed by biotin-labeling at the 3' end of in vitro transcribed RNA using the RNA 3' End Desthiobiotinylation kit (Pierce). Further details are available in the Supplementary Methods (available online).

Data Access

The raw data of microarray analysis are deposited in the Gene Expression Omnibus (GEO) under accession number GSE39846. Primary data of Nanostring gene expression analysis are deposited in the GEO under accession number GSE39077. Sequence information of MYCLos is available in GenBank (Accession number: MYCLo-1, JX046909; MYCLo-2, JX046910; MYCLo-3 v1, JX046911; MYCLo-3 v2, JX628584).

Liquid Chromatography-Tandem Mass Spectrometry (LC-MS/MS)

LC-MS/MS was performed by the Campus Chemical Instrument Center (CCIC) Mass Spectrometry and Proteomics Facility at The Ohio State University (OSU). Sample preparation and mass spectrometry are fully described in the Supplementary Methods (available online). Briefly, capillary-liquid chromatography tandem mass spectrometry (Cap-LC/MS/MS) was performed on a Thermo Finnigan LTQ mass spectrometer equipped with a CaptiveSpray source (Bruker Michrom Billerica, MA) operated in positive ion mode. The LC system was an UltiMate 3000 system from Dionex (Sunnyvale, CA). Capillary-liquid chromatography-nanospray tandem mass spectrometry (Capillary-LC/MS/MS) of global protein identification was performed on a Thermo Finnigan LTQ orbitrap mass spectrometer equipped with a microspray source (Michrom Bioresources Inc., Auburn, CA) operated in positive ion mode. Samples were separated on a capillary column (0.2X150mm Magic C18AQ 3μ 200A, Michrom Bioresources Inc, Auburn, CA) using an UltiMate 3000 HPLC system from LC-Packings A Dionex Co (Sunnyvale, CA).

Statistical Analysis

All graph values represent means ± SD from three independent experiments with each measured in triplicate. The differences between two groups were analyzed with the unpaired two-sided Student's *t* test. A *P* value of less than .05 was considered statistically significant and indicated with asterisks, as described in figure legends. The Kaplan-Meier method was used to estimate survival curves, and the log-rank test was used to test for differences between curves using SPSS Statistical Software (SPSS Inc., Chicago, IL). All statistical tests were two-sided.

Results

Identification of lncRNAs Dysregulated in CRC

To identify lncRNAs that are dysregulated in colorectal cancer, we employed a lncRNA microarray to profile lncRNAs in normal colon-derived and CRC-derived cells and tissues. From the microarray analysis covering 30 215 protein-coding transcripts and 33 045 annotated and/or known lncRNAs, we observed that a similar percentage (7%) of protein-coding transcripts (2212 of 30215) and lncRNAs (2325 of 33045) are differentially expressed ($P < .05$, greater than two-fold) in CRC (Figure 1, A and B; Supplementary Table 1, available online). Of the identified 2325 lncRNAs (1265 upregulated and 1060 downregulated lncRNAs in CRC) (Figure 1C), we selected top candidates with our criteria (greater than 15-fold change and $P < .01$) and then performed 5' and 3' rapid amplification of cDNA ends (RACE) (Supplementary Figure 1, A and B, available online). Based on the sequence information from RACE, we tested the expression levels of the lncRNAs by using quantitative real-time PCR analysis in CRC cells and tissues. Of the selected lncRNAs, four lncRNAs named *CCAT3*, *CCAT4*, *CCAT5*, and *CCAT6* (also named *MYCLo-2*) are upregulated in CRC cell lines (Figure 1, D-G; Supplementary Figure 1C, available online), and two lncRNAs named *CCAT7* and *CCAT8* are downregulated in CRC cell lines (Figure 1, H and I; Supplementary Figure 1C, available online). The results were also confirmed by using 52 CRC tissues and their matched NATs (Figure 1, J-O).

Further Identification and Characterization of a Subset of CRC-Associated lncRNAs That Are Regulated by Proto-Oncogene MYC

We tested MYC mRNA levels in multiple normal colorectal cell lines (CCD-18Co, CCD-33Co, CCD-112CoN, CCD-841CoN), CRC-derived cell lines (HT29, SW620, HCT116, RKO), CRC tissues, and their matched NATs that were used in lncRNA microarray (Figure 1, A and B). As previously reported (16), *MYC* mRNA levels were statistically significantly higher in the CRC samples than in the normal colon samples (CCD18-Co, mean = 1, SD = .00925; HCT116, mean = 17.21, SD = .40947; $P = .0025$) (Figure 2A). This result suggests that MYC could be involved in the regulation of a cohort of lncRNAs that are dysregulated in CRC (Figure 1B).

To further identify MYC-regulated lncRNAs among the lncRNAs dysregulated in CRC, we screened lncRNAs in CRC-derived cells treated with MYC-targeting siRNAs (siMYC) by using the lncRNA microarray (Supplementary Figure 2A, available online). As a result ($P < .05$, greater than two-fold), we identified 324 MYC-regulated lncRNAs in HCT116 cells (Figure 2B; Supplementary Table 2, available online) and 863 MYC-regulated lncRNAs in RKO cells (Figure 2C; Supplementary Table 3, available online). To find out the most interesting candidates that are regulated by MYC and dysregulated in CRC, we compared the lists of lncRNAs differentially expressed in CRC-derived cells (Figure 1B), siMYC-treated HCT116 cells (Figure 2B), and siMYC-treated RKO cells (Figure 2C). By selecting lncRNAs commonly found in the three groups, we finally isolated three lncRNAs (AK021907, AC074389.9, and *KTN1-AS1*) upregulated by MYC

ARTICLE

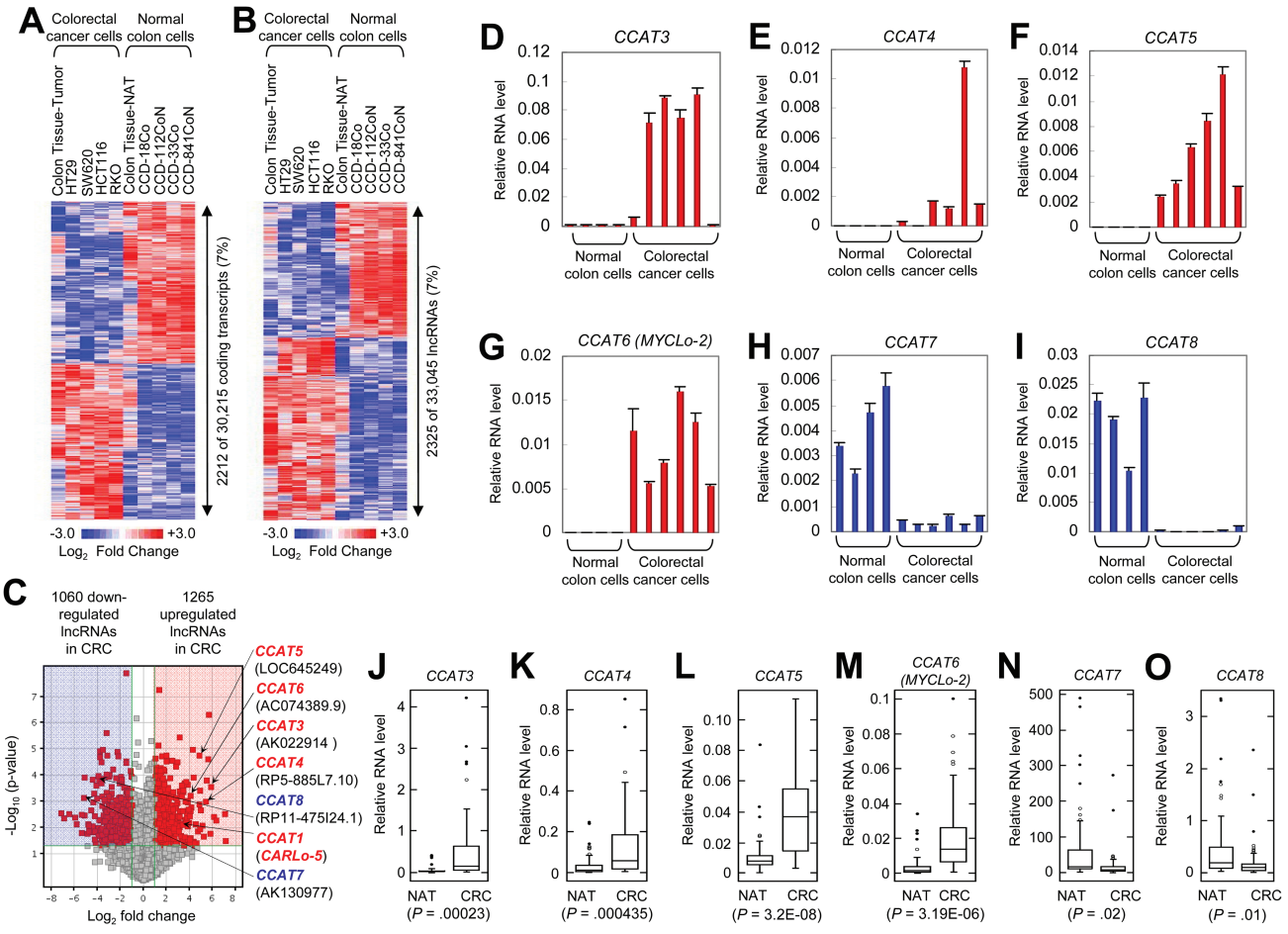

Figure 1. Identification of long noncoding RNAs (lncRNAs) differentially expressed in colorectal cancer (CRC). **A and B)** Heatmaps of protein-coding transcripts **(A)** and lncRNAs **(B)** dysregulated in CRC (HCT116, RKO, SW620, HT29, and CRC tissues), compared with normal colon (CCD-18Co, CCD-33Co, CCD112CoN, CCD-841-CoN and colon normal adjacent tissues [NATs]). **C)** Volcano map indicating up- or downregulation of CRC-associated lncRNAs (CCAT1, CCAT3~8). **D-G)** Verification of induced expression of *CCAT3* (D), *CCAT4* **(E)**, *CCAT5* **(F)**, and *CCAT6* **(G)** in CRC cell lines by using quantitative real-time polymerase chain reaction (qRT-PCR). Data are means ± SD of three independent experiments and each measured in triplicate. **H and I)** Verification of repressed expression of *CCAT7* **(H)** and *CCAT8* **(I)** in CRC cell lines by using qRT-PCR. Data are means ± SD of three independent experiments and each measured in triplicate. **J-O)** Differential expression of *CCAT3* **(J)**, *CCAT4* **(K)**, *CCAT5* **(L)**, *CCAT6* **(M)**, *CCAT7* **(N)**, and *CCAT8* **(O)** in 52 matched CRC and NAT tissues. Shown are **box plots** with **lower and upper bounds of the boxes** representing the 25th and 75th quartiles, respectively; **whiskers** demarcate values within the 10th to 90th percentiles, and **solid circles** indicate values less than the 10th percentile and greater than the 90th percentile.

(Figure 2D). These MYC-regulated lncRNAs are named *MYCLos* (AK021907, *MYCLo-1*; AC074389.9 [*CCAT6*], *MYCLo-2*; KTN1-AS1, *MYCLo-3*). Of the three lncRNAs, *MYCLo-2* is identical with *CCAT6* that we identified and verified as the lncRNA upregulated in CRC (Figure 1, G and M; Supplementary Figure 1B, available online).

By using 5' and 3' rapid amplification of cDNA ends (RACE), we determined the presence and full length of the MYC-regulated lncRNAs (Supplementary Figure 2B, available online; *MYCLo-2* is shown in Supplementary Figure 1B, available online). The expression of the lncRNAs was also confirmed by Northern blot (Supplementary Figure 2C, available online). The results show that actual sequences of the lncRNAs are a little different from the predicted sequences (Supplementary Figure 2D, available online) and MYCLos are localized in various genomic loci such as chromosome 20, 7 and 14 (Supplementary Figure 2, E-G, available online).

We next determined if MYC-mediated regulation of the *MYCLos* is common in various types of cancer cells. MYC-mediated regulation of *MYCLos* was observed in the cells from various cancer types, indicating that MYC-mediated regulation of *MYCLos* is conserved in many types of cancer and suggesting a universal role of these lncRNAs in various MYC-driven cancer cells (Figure 2, E-G). By using an additional siRNA-targeting MYC, we confirmed the MYC-mediated regulation of the *MYCLos* (Supplementary Figure 2, H and I, available online).

To further verify the relationships between MYC and MYCLos, we also examined their expression levels in 50 human primary colorectal tissue samples (25 normal colon and 25 CRC tissue samples) classified into four groups by *MYC* expression level (Figure 2H). By comparing the expression levels of *MYCLo-1*, *-2*, and *-3* in the four groups, we found that expression levels of *MYCLo-1*, *-2*, and *-3* are statistically significantly associated with *MYC* expression level (Figure 2, I-K). In addition, *MYCLos* are highly expressed in CRC cell lines (Figure 1G; Supplementary Figure 2, J and K, available online) that harbor MYC overexpression (Figure 2A).

To test whether MYC regulates *MYCLo-1*, *-2*, and *-3* at the transcription level, we exploited a luciferase reporter assay. The promoter activities of the *MYCLos* were reduced by *MYC* knockdown, indicating that MYC induces the *MYCLos* expression at the transcription level (Figure 2, L-N). Using the database of open chromatin TFBS by ChIP-seq from ENCODE/Open Chrom

ARTICLE

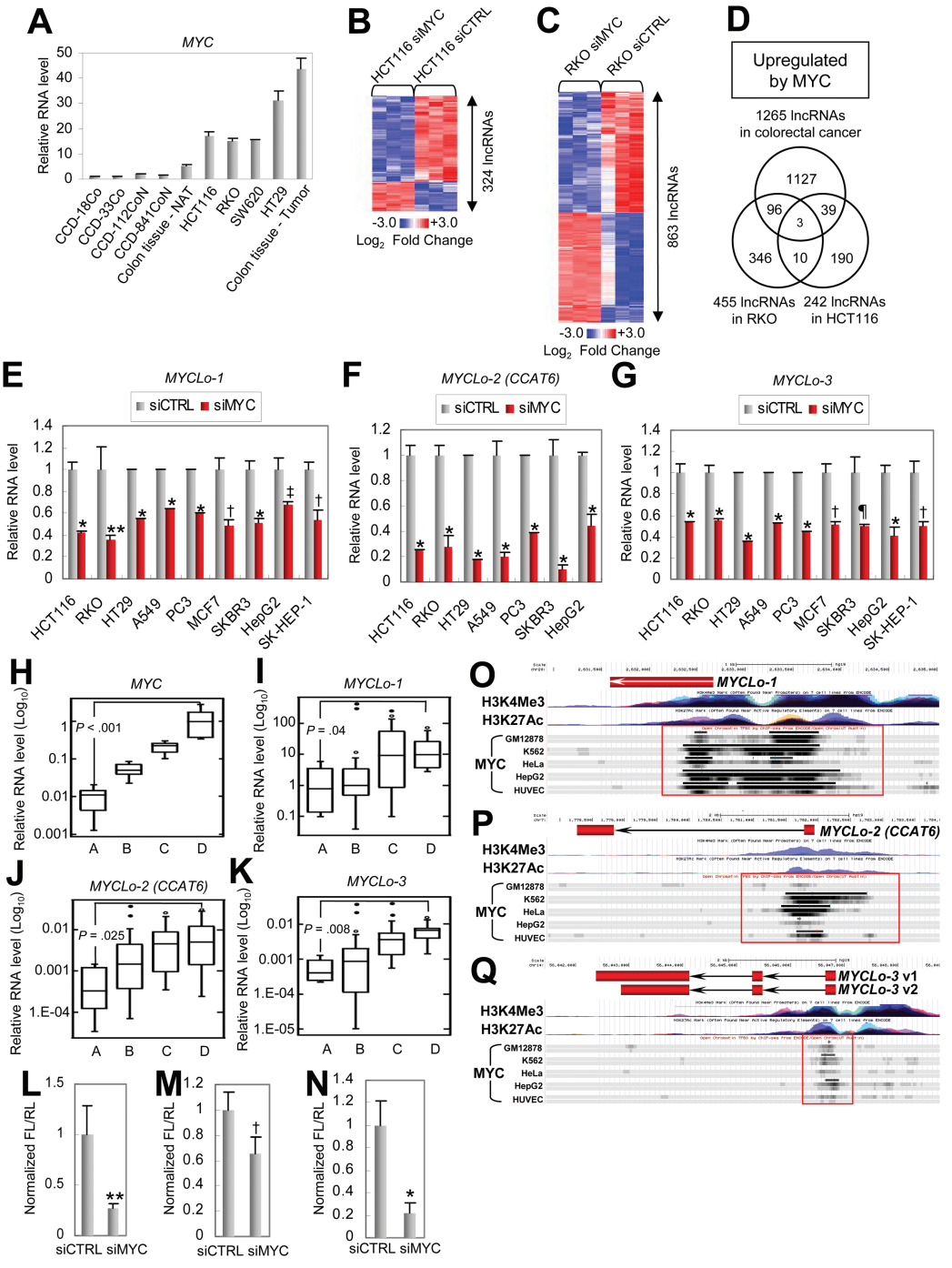

Figure 2. Identification of colorectal cancer [CRC]–associated lncRNAs directly regulated by MYC. **A)** Comparison of mRNA levels of *MYC* in normal colon–derived (CCD-18Co, CCD-33Co, CCD112CoN, CCD-841-CoN, and colon normal adjacent tissue [NAT] samples) and CRC cells/tissues (HCT116, RKO, SW620, HT29, and CRC tissue samples). Data are means ± SD of three independent experiments and each measured in triplicate. **B and C)** Heatmaps of lncRNAs dysregulated by MYC knockdown in HCT116 **(B)** and RKO **(C)**. **D) Venn diagrams** showing the number of upregulated long noncoding RNAs (lncRNAs) in a MYC-dependent manner. Hypergeometric probability of three lncRNAs commonly found in all criteria is $P(X=3) = 0.01$. **E-G)** Quantitative real-time polymerase chain reaction (qRT-PCR) results showing MYC-mediated positive regulation of *MYCLo-1* **(E)**, -2 **(F)**, and -3 **(G)** in various types of cancer cells. Data are means ± SD of three independent experiments and each measured in triplicate (**P = .0062; †P = .001; ‡P = .0079; ¶P = .004; *P < .001). Statistical significance determined by unpaired two-sided Student's *t* test. **H-K)** Expressional associations between *MYC* **(H)** and *MYCLos* (*MYCLo-1* **[I]**, -2 **[J]**, and -3 **[K]**) in 50 colorectal tissue samples. The number of samples in each group is eight (Group A), 17 (Group B), 15 (Group C), and 10 (Group D). The *P* values between Group A and Group D are indicated. Shown are **box plots** with **lower and upper bounds of the boxes** represent the 25th and 75th quartiles, respectively; **whiskers** demarcate values within the 10th to 90th percentiles, and **solid circles** indicate values less than the 10th percentile and greater than the 90th percentile. Statistical significance was determined by the unpaired two-sided Student's *t* test. **L-N)** Luciferase assays showing MYC-dependent regulation of 5' promoter activities of *MYCLo-1* **(L)**, -2 **(M)**, and -3 **(N)**. The promoter region of each MYCLo for luciferase assay is indicated with a **red box** in **(O-Q)**, respectively. Data are means ± SD of three independent experiments and each measured in triplicate (**P = .01; †P = .03; *P = .004). Statistical significance was determined by the unpaired two-sided Student's *t* test. **O-Q)** The database of open chromatin TFBS by ChIP-seq from ENCODE/Open Chrom (UT Austin) shows that MYC binds to 5' promoter regions of *MYCLo-1* **(O)**, -2 **(P)**, and -3 **(Q)** in various types of cells such as GM12878, K562, HeLa, HepG2, and HUVEC. MYC-binding regions are indicated with **red boxes**.

ARTICLE

(UT Austin) (17), we also observed strong and common binding of MYC to the promoters of the *MYCLo*s in various cells (Figure 2, O-Q). These results suggest that the MYC-induced *MYCLo*s are directly regulated by the transcription enhancer MYC at the transcription level.

Effect of MYC-Induced MYCLos on Cell Proliferation and Expression of MYC Target Genes Such as *CDKN1A* and *CDKN2B*

The proto-oncogene *MYC* accelerates cell proliferation by regulating many cell cycle regulator genes (10). To determine whether MYC-induced *MYCLo*s are involved in the MYC function, the effect of MYCLos in cell proliferation was examined using siRNAs targeting *MYCLo*s (siMYCLos). In HCT116 (colorectal cancer) and PC3 (prostate cancer) cells, knockdown of *MYCLo-1*, *-2*, or *-3* as well as *MYC* resulted in decreased cell proliferation (siCTRL, 3.63056 ± 0.20821, siMYCLo-2, 2.61959 ± 0.0482, $P < .001$) (Figure 3A) (siCTRL, 3.94523 ± 0.2959, siMYCLo-2, 3.07757 ± 0.26933, $P = .0048$) (Figure 3B). In addition, we exogenously introduced the MYC-induced *MYCLo*s to confirm their function in cell proliferation (Supplementary Figure 3A, available online). Consistent with the knockdown experiments, overexpression of the *MYCLo*s in normal colon-derived fibroblasts resulted in enhanced cell proliferation (siCTRL, 2.77902 ± 0.13299, siMYCLo-2, 3.56119 ± 0.18969, $P < .001$) (Figure 3C). These results indicate that the MYC-induced *MYCLo*s such as *MYCLo-1*, *-2*, and *-3* are supportive to MYC function by enhancing cell proliferation.

MYC enhances cell cycle progression by regulating cell cycle arrests, leading to an increase of cell proliferation rate (10). To investigate if *MYCLo*s also have a function in cell cycle regulation, we analyzed the proportion of cell populations in each cell cycle phase (G1, S, and G2). Knockdown of *MYCLo-1* or *-2* resulted in accumulation of cells in the G1 phase, suggesting that *MYCLo-1* and *-2* are involved in the G1/S transition (Figure 3D). Knockdown of *MYCLo-3* led to accumulation of cells in the S and G2 phases, suggesting the function of *MYCLo-3* in G2 phase regulation (G1 phase, siCTRL, 64.58 ± 0.34771, siMYCLo-1, 77.97333 ± 0.70501, $P < .001$, siMYCLo-2, 73.00667 ± 0.4517, $P < .001$, siMYCLo-3, 59.25 ± 0.42884, $P < .001$, siMYC, 74.32333 ± 0.97552, $P < .001$; S phase, siCTRL, 18.82 ± 0.4613, siMYCLo-1, 12.11333 ± 0.50501, $P < .001$, siMYCLo-2, 13.95 ± 0.5656, $P < .001$, siMYCLo-3, 20.55333 ± 0.82779, $P = .047$, siMYC, 12.93667 ± 1.26508, $P < .0085$; G2 phase, siCTRL, 15.85667 ± 0.35233, siMYCLo-1, 8.59333 ± 0.02887, $P < .001$, siMYCLo-2, 11.82 ± 0.31512, $P < .001$, siMYCLo-3, 10.35667 ± 0.37634, $P = .00662$, siMYC, 18.80667 ± 0.67419, $P < .001$) (Figure 3D).

To identify cell cycle regulator genes modulated by the MYC-induced *MYCLo*s (*MYCLo-1*, *-2*, and *-3*), we used nCounter Virtual Cell Cycle Gene Sets of the NanoString Gene Expression Assay. Of 183 cell cycle regulator genes, a cohort of genes were detected as downstream genes of MYCLos ($P < .05$, greater than 1.5-fold change): 19 genes regulated by MYCLo-1 (Figure 3E; Supplementary Table 4-2, available online), 49 genes regulated by MYCLo-2 (Figure 3F; Supplementary Table 4-3, available online), and 13 genes regulated by MYCLo-3 (Supplementary Figure 3B and Supplementary Table 4-4, available online). We also found a subset of genes that are commonly regulated by MYC and the MYCLos, by profiling cell cycle regulator genes dysregulated by *MYC* knockdown (Supplementary Figure 3C and Supplementary Table 4-1, available online).

Using qRT-PCR, we confirmed that elevated expression levels of *CDKN1A* and *CDKN2B* by knockdown of *MYCLo-1* or *-2* as well as *MYC* knockdown (Figure 3, G and H, left and middle panels; Supplementary Figure 3D, available online). We further verified a few more cell cycle regulator genes such as *YWHAB* (14-3-3 alpha), *SFN* (14-3-3 sigma), and *CFN* (cofilin) that are also regulated by MYC and MYCLo-2 (Figure 3H, middle panel). These elevations are consistent with the effect of *MYC* knockdown, albeit independent of *MYC*, *Miz-1*, and p53 expression levels (Figure 3, G and H, right panels; Supplementary Figure 3D, available online).

MYCLos-Mediated Transcriptional Regulation of CDKN1A and CDKN2B in the Distal Promoter Regions

To demonstrate the mechanism by which the MYC-regulated lncRNAs repress *CDKN1A* and *CDKN2B* expression, we amplified two different regions in the promoters of *CDKN1A* and *CDKN2B* genes, respectively, one including the proximal MYC-binding (MB) region and the other including the upstream region without the MB region (Supplementary Figure 4, A and B, available online), and exploited the amplified regions for testing promoter activity using a luciferase reporter assay (Figure 4, A and B; Supplementary Figure 4, C and D, available online).

We first sought to test if MYCLo-1 and -2 are involved in the transcriptional regulation of *CDKN1A* and *CDKN2B* in the proximal MB regions on which MYC binds with the other MYC-associated factors. Knockdown of MYC induced promoter activities of *CDKN1A* and *CDKN2B* genes; however, their promoter activities were not statistically significantly affected by knockdown of *MYCLo-1* or *-2* (Supplementary Figure 4, C and D, available online). Interestingly, the knockdown of *MYC* also induced their promoter activities in the distal promoter regions without the MB region, and knockdown of *MYCLo-1* or *-2* also induced the promoter activities of *CDKN1A* and/or *CDKN2B* (Figure 4, A and B, available online). These results indicate that MYC can control transcription activity of *CDKN1A* and *CDKN2B* not only in the proximal region but also in the distal regions of their promoters. In addition, the results also demonstrate that MYCLo-1 and -2 are implicated in the MYC-regulated transcription activity of *CDKN1A* and *CDKN2B* genes in their distal promoter regions.

To further identify the specific promoter regions of *CDKN1A* and *CDKN2B* regulated by MYCLo-1 and -2, we serially deleted the promoter region from the distal side and tested their promoter activities (Figure 4, C and D, left panels). The luciferase reporter assay using the deleted genomic regions of *CDKN1A* promoter indicated that the *CDKN1A* promoter region approximately between -2768bp and -2480bp is critical for *CDKN1A* regulation by MYCLo-1 (Figure 4 C). The luciferase reporter assay using the deleted genomic regions of *CDKN2B* promoter also demonstrated that the *CDKN2B* promoter region approximately between -840bp and -570bp is critical for *CDKN2B* regulation by MYCLo-2 (Figure 4 D). These results reveal the specific promoter regions that involve MYCLos in the MYC-mediated transcriptional regulation of *CDKN1A* and *CDKN2B*.

Role of Physical Interactions Between MYCLos and RNA Binding Proteins Such as HuR and hnRNPK

To investigate the mechanism by which MYCLos function, we sought to identify the RNA-binding proteins for MYCLo-1 and -2 using RNA pull-down assays. By incubating biotinylated RNA or antisense RNA of the MYCLos with streptavidin beads and nuclear cell extracts, we isolated proteins specifically associated with MYCLo-1 or -2 and resolved them on an SDS-PAGE gel followed by mass spectrometry of the RNA-associated

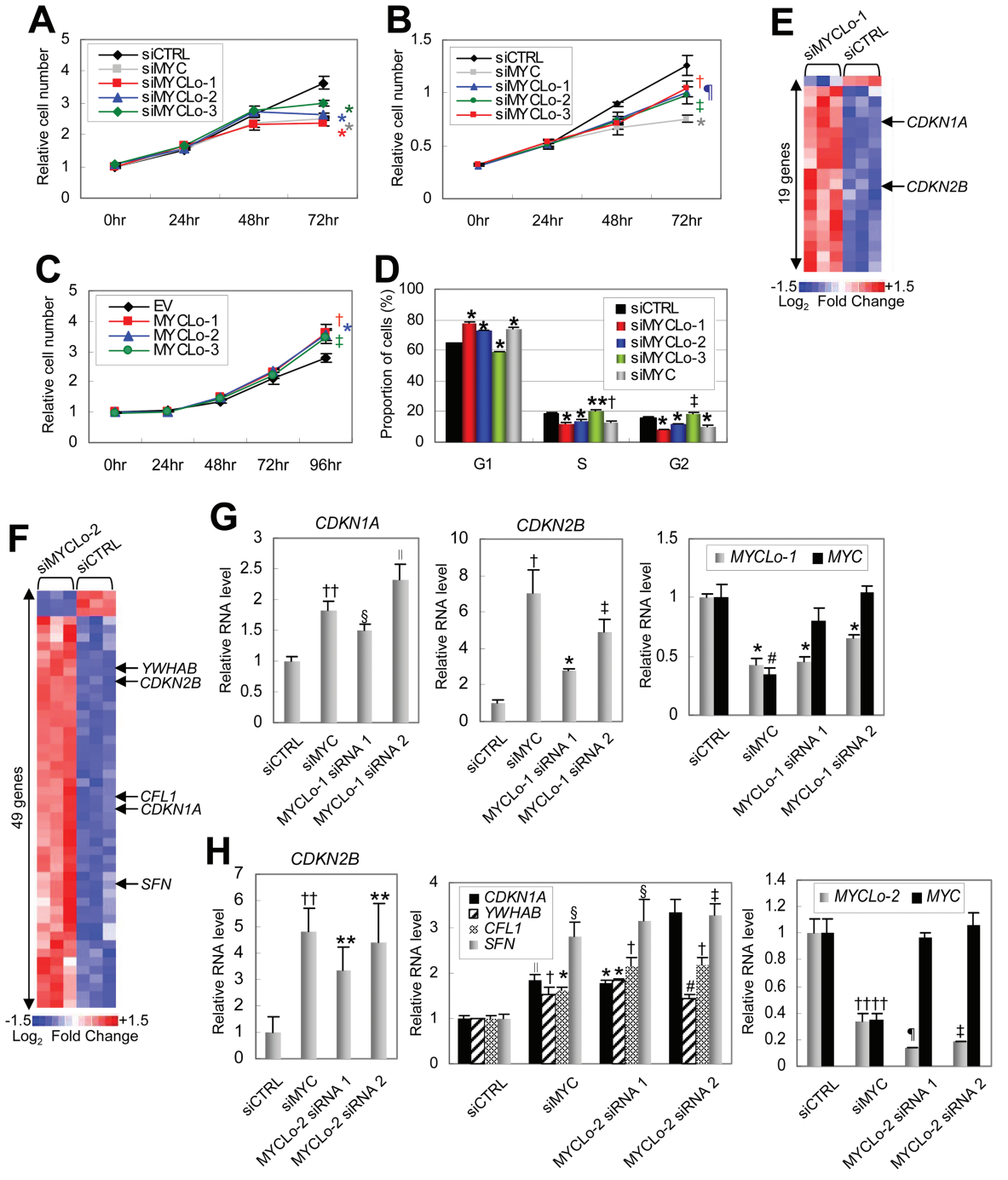

Figure 3. Effect of *MYCLo*s knockdown on cell proliferation and cell cycle progression. **A and B)** Cell proliferation assays. HCT116 (n = 5, A) or PC3 (n = 4, B) cells were treated with siRNAs (final concentration: 50 nM), as indicated and subjected to proliferation assay every 24 hours (†P = .013; ‡P = .0048; ¶P = .009; *P < .001). **Error bars** represent standard deviation. **C)** Cell proliferation assay. CCD-18Co cells were transfected with pcDNA3.3 plasmids (EV) expressing *MYCLo*-1, -2, or -3 and subjected to a cell proliferation assay every 24 hours (n = 3) (*P = .001; †P = .0045; ‡P = .0025). **Error bars** represent standard deviation. **D)** Proportion of cells in each cell cycle phase determined by flow cytometry analysis. HCT116 cells were treated with siRNAs (50 nM) as indicated and analyzed 48 hours after transfection. Data are mean ± SD of three independent experiments and each measured in triplicate (**P = .047; †P = .0085; ‡P = .00662; *P < .001). **E)** Heatmap representing cell cycle regulator genes dysregulated by MYCLo-1. The genes that are commonly regulated by MYC are indicated. Expression values displayed in gradient of **red** and **blue** are Log2-transformed fold change. The list of the dysregulated genes is available in Supplementary Table 4 (available online). **F)** Heatmap representing cell cycle regulator genes dysregulated by MYCLo-2. The genes that are commonly regulated by MYC are indicated. Expression values displayed in gradient of **red** and **blue** are Log2-transformed fold change. The list of the dysregulated genes is available in Supplementary Table 4 (available online). **G)** Quantitative real-time polymerase chain reaction (qRT-PCR) results showing MYC-independent regulation of *CDKN1A* (**left**) and *CDKN2B* (**middle**) expression by *MYCLo*-1 knockdown (**right**). HCT116 cells were treated with 50 nM siRNAs targeting *MYC* or *MYCLo*-1 for 72 hours. Data are mean ± SD of three independent experiments, measured in triplicate (††P = .003; §P = .0017; ‖P = .013; †P = .013; ‡P = .001; #P = .002; *P < .001). **H)** qRT-PCR results showing MYC-independent regulation of *CDKN2B* (**left**), *CDKN1A*, *YWHAB*, *CFL1*, and *SFN* (**middle**) expression by *MYCLo*-2 knockdown (**right**). HCT116 cells were treated with 50 nM siRNAs targeting *MYC* or *MYCLo*-2 for 72 hours. Data are mean ± SD of three independent experiments and each measured in triplicate (**P = .03; ††P = .002; ‖P = .003; §P = .01; †P = .001; ‡P = .005; #P = .016; ¶P = .004; *P < .001). Statistical significance was determined by the unpaired two-sided Student's *t* test.

ARTICLE

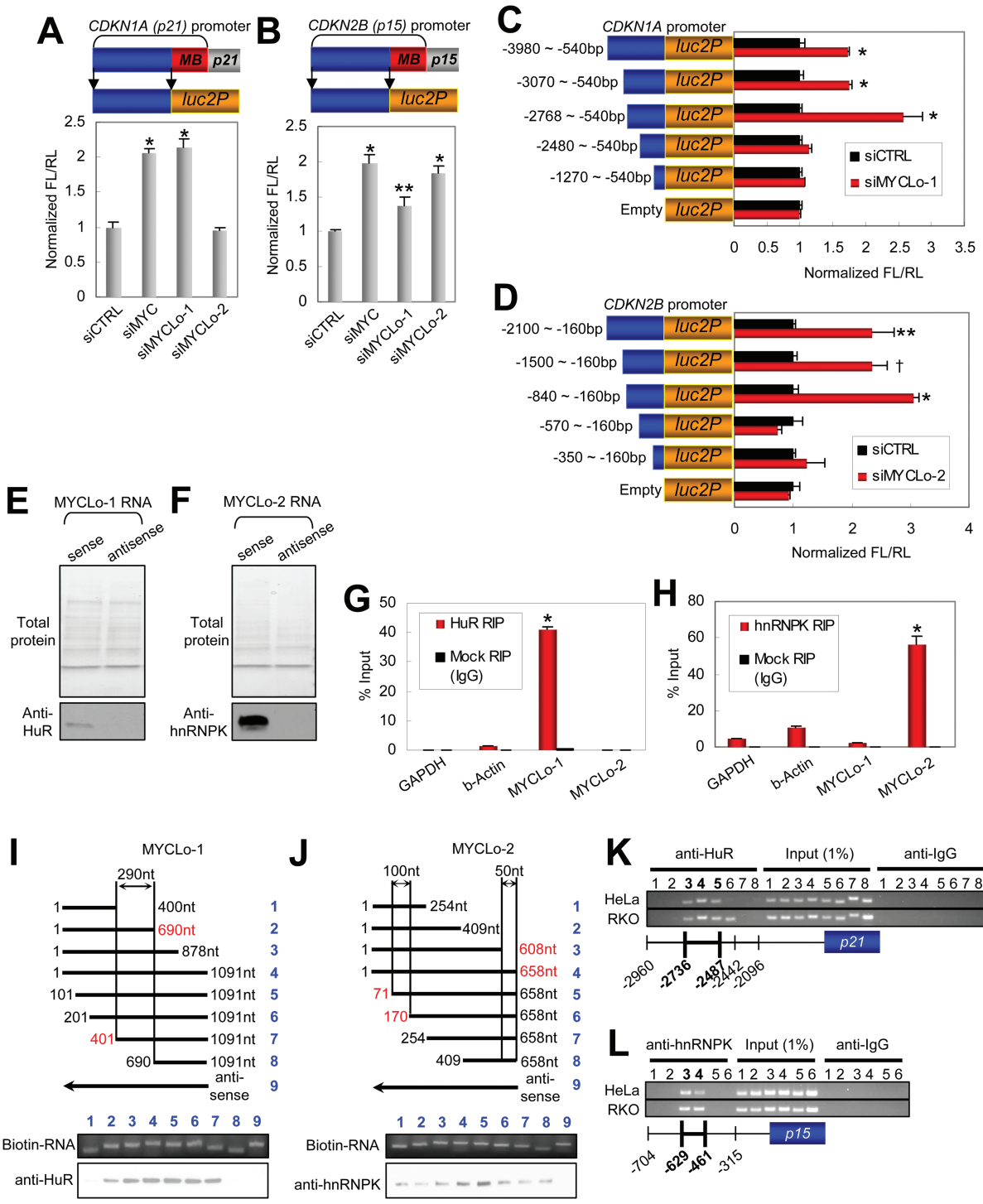

Figure 4. Interactions between MYCLo-1/2 and RNP binding proteins (HuR and hnRNPK) and their involvement in the regulation of 5' promoter activities of *CDKN1A* and *CDKN2B*. **A and B)** Schematics (**top**) of pGL4 luciferase vectors inserted with distal 5' promoter regions (**blue bars**) of *CDKN1A* **(A)** and *CDKN2B* **(B)**. **Red bars** depict proximal promoter regions where MYC binds (MB). Luciferase reporter assays (**bottom**) representing transcription activity of the distal 5' promoter regions of *CDKN1A* **(A)** and *CDKN2B* **(B)** in HCT116 cells transfected with the pGL4 luciferase vectors and siRNAs as indicated. Data are mean ± SD of three independent experiments and each measured in triplicate (**P = .024; *P < .001). **C and D)** Luciferase reporter assays to identify specific 5' promoter regions of *CDKN1A* **(C)** and *CDKN2B* **(D)**, where MYCLo-1 and -2 regulate their promoter activities, respectively. Data are mean ± SD of three independent experiments and each measured in triplicate (**P = .027; †P = .014; *P < .001). **E and F)** RNA pull-down assays showing the interactions between MYCLo-1 and HuR **(E)**, and MYCLo-2 and hnRNPK **(F)**. Total protein in SDS-PAGE gel was analyzed by liquid chromatography–tandem mass spectrometry. Western blot data are representative of two independent experiments. **G and H)** RIP assays and quantitative real-time polymerase chain reaction detection demonstrating the specific interactions between HuR and MYCLo-1 **(G)**, and hnRNPK and MYCLo-2 **(H)**. Data are mean ± SD of three independent experiments and each measured in triplicate (*P < .001). **I and J)** Deletion mapping analyses showing the importance of central region of MYCLo-1 (I, 401~690 bp) and of marginal regions of MYCLo-2 (J, 71~170 bp and 608~658 bp) in the interactions with HuR and hnRNPK, respectively. Data are representative of three independent experiments. **K and L)** ChIP assays showing that HuR binds to the specific 5' promoter region of *CDKN1A*, where MYCLo-1 regulates its transcription activity **(K)** and that hnRNPK binds to the specific 5' promoter region of *CDKN2B*, where MYCLo-2 regulates its transcription activity **(L)**. Data are representative of three independent experiments.

ARTICLE

total proteins (Figure 4, E and F, upper panels). As a result, we identified 10 proteins associated with MYCLo-1 and 8 proteins associated with MYCLo-2 (Supplementary Figure 4, E and F, available online). Of the identified proteins, we found RNA-binding protein ELAVL1 (HuR) in the MYCLo-1 pull-down assay (Supplementary Figure 4E, available online). In addition, we found hnRNPK and hnRNPR as RNA-binding proteins interacting with MYCLo-2 (Supplementary Figure 4F, available online). The counted number of peptides indicates that MYCLo-2 more preferentially interacts with hnRNPK (46 peptides) than hnRNPR (6 peptides) (Supplementary Figure 4F, available online). By using an RNA-Protein Interaction Prediction program (RPISeq) (18), we also observed the high probability of HuR-MYCLo-1 and hnRNPK-MYCLo-2 interactions (Figure 4, G and H). The interactions were also verified by using Western blot analysis (Figure 4, E and F, lower).

To further confirm the interactions (HuR-MYCLo-1 and hnRNPK-MYCLo-2), we conducted RNA immunoprecipitation (RIP) using antibodies against HuR or hnRNPK. Consistent with the results of RNA pull-down assay, MYCLo-1 is abundant in RIP samples using HuR antibodies as compared with the samples using nonspecific (negative control using IgG antibody) antibodies (Figure 4G), and MYCLo-2 is enriched by RIP using hnRNPK antibodies (Figure 4H). To determine which specific regions of MYCLo-1 and -2 interact with HuR or hnRNPK, we performed deletion-mapping experiments using truncated MYCLo-1 or MYCLo-2 (Figure 4, I and J, upper panels). The analyses suggest that HuR interacts with the central region (401~690bp) of MYCLo-1 (Figure 4I, lower panel). On the other hand, the various 5' or 3' deletions of MYCLo-2 do not affect the interaction between MYCLo-2 and hnRNPK (Figure 4J, lower panel). However, the enrichment of hnRNPK in full-length (#4) and partially deleted (#5, deleted in 1-70nt) RNAs of MYCLo-2 suggests that hnRNPK might interact with at least two regions of MYCLo-2 (71-170nt and 608-658nt). The prediction analysis (RPISeq) using the sequence of the central regions of MYCLo-1 and -2 also shows that the regions are strongly predicted to interact with the RNA-binding proteins, supporting the conclusion (Supplementary Figure 4, G and H, available online).

We identified the specific regions in the promoters of *CDKN1A* (-2768bp~-2480bp) and *CDKN2B* (-840bp~-570bp) genes that implicate MYCLo-1 and -2 in transcriptional regulation of the genes (Figure 4, C and D). To determine whether MYCLo-1/HuR and MYCLo-2/hnRNPK complexes are involved in the regulation at the specific promoter regions by direct interaction, we performed a chromosome immunoprecipitation (ChIP) assay. By using antibodies against HuR, we observed that HuR interacts with the specific region (-2736bp~-2487bp) in the promoter of *CDKN1A* (Figure 4K). The result of the ChIP assay using antibodies against hnRNPK also shows that hnRNPK interacts with the specific region (-629bp~-461bp) of the *CDKN2B* promoter (Figure 4L). The coincidence of MYCLos function and HuR/hnRNPK binding strongly suggests that HuR is implicated in the transcriptional repression of *CDKN1A* through interaction with MYCLo-1 and that MYCLo-2 represses *CDKN2B* transcription by interacting with hnRNPK.

Oncogenic Function of MYCLo-2

By using northern blot, we confirmed the overexpression of *MYCLo-2* (*CCAT6*) in CRC cell lines (Supplementary Figure 5A, available online). In addition, the comparison of individual pairs of the tissue samples clearly shows that most CRC tissues harbor very high expression levels of *MYCLo-2* and that *MYCLo-2* is more highly expressed in 46 CRC tissues of the 52 pairs of the matched tissue samples (Figure 5A). In addition, *MYCLo-2* is also overexpressed in PC cells and tissues, compared with normal prostate-derived cells (Figure 5, B and C).

The knockdown of *MYCLo-2* statistically significantly reduced the number of cells and colonies in colony formation assays in vitro, indicating that MYCLo-2 has a role in tumor cell transformation (HCT116 cell number, siCTRL, 1 ± 0.06391, siMYCLo-2-1, 0.66259 ± 0.08495, P = .0066, siMYCLo-2-2, 0.66259 ± 0.08495, P = .00315; PC3 cell number, siCTRL, 1 ± 0.02433, siMYCLo-2-1, 0.62727 ± 0.08494, P = .01185, siMYCLo-2-2, 0.6278 ± 0.04929, P = .00151; HCT116 colony number, siCTRL, 100 ± 23.52415, siMYCLo-2-1, 53.90625 ± 23.85053, siMYCLo-2-2, 48.4375 ± 6.50521; PC3 colony number, siCTRL, 100 ± 28.11947, siMYCLo-2-1, 34.04255 ± 15.53823, siMYCLo-2-2, 44.68085 ± 8.14832) (Figure 5D; Supplementary Figure 5B, available online). We also examined the knockdown effect of MYCLo-2 in tumorigenesis by using in vivo xenografts of tumor cells transfected with *MYCLo-2* siRNAs. Consistent with our data supporting the oncogenic function of *MYCLo-2*, tumor development was statistically significantly inhibited by MYCLo-2 depletion in both CRC-derived (HCT116) and PC-derived (PC3) cells (Figure 5E; Supplementary Figure 5C, available online). These results demonstrate that *MYCLo-2* is not only overexpressed in tumors but also involved in tumorigenesis and tumor growth.

Discussion

In this work, we identified novel lncRNAs differentially regulated in CRC by profiling CRC cells and tissues. In addition, MYC-regulated lncRNAs named *MYCLos* were further identified. *MYCLos* participate in cell proliferation and cell cycle regulation by modulation of expression of known MYC target genes such as *CDKN1A* and *CDKN2B*. We further found that MYCLo-1 physically interacts with HuR and MYCLo-2 with hnRNPK. Further data support that these interactions might be involved in the regulation of MYC targets such as *CDKN1A* and *CDKN2B*. Lastly, we show that knockdown of *MYCLo-2* inhibits cancer cell transformation and tumorigenesis.

In addition to the recent studies that identified a couple of CRC-associated lncRNAs such as CCAT1 and CCAT2, we discovered and verified more novel CRC-associated lncRNAs (7–9). In addition, we identified the lncRNAs that are downregulated in CRC, suggesting their putative tumor suppressor function. The up- or downregulation of a newly identified lncRNA named CCAT3-8 suggests the function of lncRNAs in CRC. Furthermore, the dysregulation of CCAT3-8 in CRC tissue samples supports our suggestion for putative function of CCAT3-8 in cancer pathogenesis. Indeed, our results show that CCAT6 (MYCLo-2) have a role in oncogenesis. To elucidate the oncogenic or tumor-suppressive function of other lncRNAs, further studies are required.

By further identification of MYC-regulated lncRNAs in CRC-associated lncRNAs, we also revealed an unknown mechanism of MYC function through lncRNAs. MYC-regulated lncRNAs, such as *MYCLo-1* and *MYCLo-2*, regulate known MYC target genes, such as *CDKN1A* and *CDKN2B*, through the interactions with HuR and hnRNPK. To date, many studies have reported a potential role of the RNA-binding proteins such as hnRNPK and HuR in cancer (19–21). However, no notable mechanism of their function in cancer has been reported yet. Here, our results raise the possibility that lncRNAs associated with hnRNPK or HuR might be related to their function in cancer.

Recent reports show that *CDKN1A* (p21) is a critical target gene of MYC. MYC-repressed *CDKN1A* expression is involved

ARTICLE

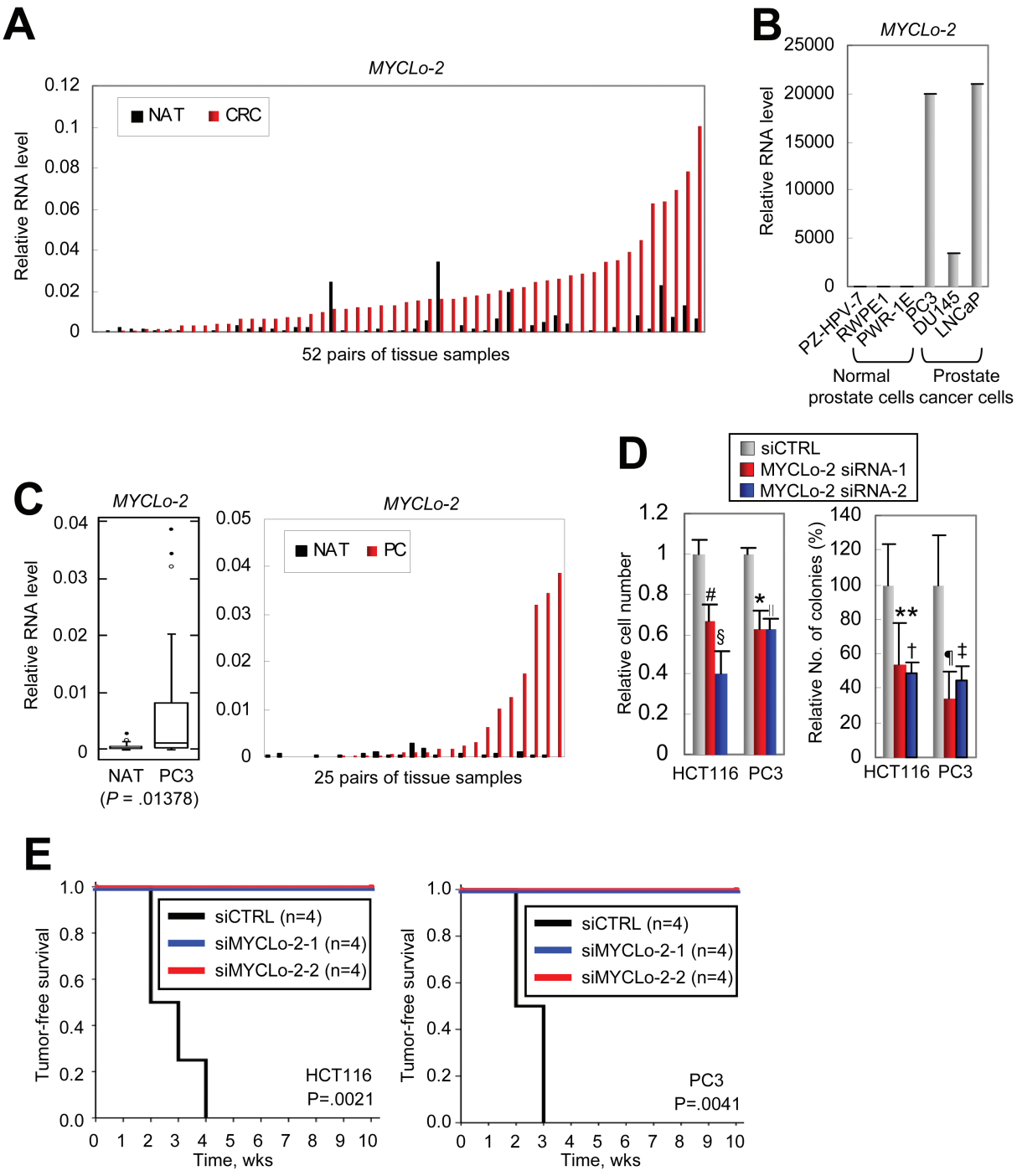

Figure 5. Function of MYCLo-2 in cancer cell transformation and tumorigenesis. **A)** Comparison of expression level of *MYCLo-2* in each pair of CRC tissues (**red**) and their matched normal adjacent tissues (NATs) (**black**). **B)** Quantitative real-time polymerase chain reaction (qRT-PCR) results showing significant overexpression of *MYCLo-2* in PC-derived cell lines, compared with normal prostate-derived cell lines. Data are mean ± SD of three independent experiments and each measured in triplicate. **C) Box and whisker plot** (**left**) showing the significant overexpression of *MYCLo-2* in PC, compared with their matched NAT (25 pairs of primary tissues). Comparison of expression level (**right**) of *MYCLo-2* in each pair of PC tissues (**red**) and their matched NATs (**black**). **D)** Soft agar colony formation assays indicating that knockdown of *MYCLo-2* causes a decreased number of cells (**left**) and colonies (**right**) in CRC-derived (HCT116) and PC-derived (PC3) cells. Data are mean ± SD of three independent experiments, each measured in triplicate (#$P = .0066$; §$P = .00315$; *$P = .01185$; ‖$P = .00151$; **$P = .003322$; †$P = .001821$; ¶$P = .0107$; ‡$P = .02474$). **E)** Kaplan-Meier plot of tumor-free survival analysis in athymic nude mice xenografted with siRNA-treated HCT116 (**left**) or PC3 (**right**) cells as indicated. The Kaplan-Meier method was used to estimate survival curves, and the log-rank test was used to test for differences between curves using SPSS Statistical Software (SPSS Inc., Chicago, IL).

in various MYC functions such as cell cycle, cell death, cellular senescence, tumorigenesis, epithelial-mesenchymal transition, and stemness (15,22–25). Our data show that MYC-regulated lncRNAs are involved in transcriptional repression of *CDKN1A*, suggesting lncRNA involvement in the versatile functions of MYC. Although we tried to establish stable knockdown cells of MYCLo-2, the cells harboring *MYCLo-2* knockdown disappeared from the mixed cell population in a couple of weeks and single

clonal cells with *MYCLo-2* knockdown were extinct, suggesting that knockdown of *MYCLo-2* inhibits cell cycle progression at the early stage; however, it may have a role in other processes such as cellular senescence and cell death.

Although we show that lncRNAs such as MYCLo-2 are regulated by MYC in a wide range of cancer types, we verified their overexpression and oncogenic function in colorectal and prostate cancer. To expand the knowledge of *MYCLo-2* in other types of cancer, further investigation is required. We identified the lncRNAs in human cancers. Therefore, their homologous lncRNAs such as *Myclos* in rodents are not yet known. For better understanding of the lncRNAs in vivo, the identification of their counterparts in rodents is highly needed. Finally, other lncRNAs identified in this study also remain to be characterized in future studies.

The transcription factor MYC is a well-known regulator of cell stemness (26). It was recently reported that dicer deficiency may cause deregulation of lncRNA through MYC dysregulation in embryonic stem cells (27). The results also support that MYC-regulated lncRNAs have a critical role not only in oncogenesis but also in other MYC functions. Although we identified and characterized several lncRNAs associated with CRC and MYC, more lncRNAs remain to be explored. Our findings suggest new targets of cancer and MYC-associated pathogenesis.

Funding

This work was supported by grants from the National Cancer Institute (EDRN U01 CA152758).

Notes

TK and CMC contributed to project coordination. TK conceived the idea. TK and YJJ designed the project. TK identified and registered *CCATs* and *MYCLos*. TK, YJJ and RC performed experiments. TK, YJJ, JHL, YP, SHK, and ET analyzed data. HA provided quantitative real-time polymerase chain reaction and NanoString Gene Expression assays data. TK and CMC prepared the manuscript.

We especially thank Dr. Robert J. Coffey (Vanderbilt University Medical Center) for the support and advice that contributed to this manuscript. We also thank Dr. Thomas D. Schmittgen (The Ohio State University) for the revision of this manuscript.

References

1. Mattick JS, Makunin IV. Small regulatory RNAs in mammals. *Hum Mol Genet*. 2005;14 Spec No 1:R121–R132.
2. Guttman M, Rinn JL. Modular regulatory principles of large non-coding RNAs. *Nature*. 2012;482(7385):339–346.
3. Khalil AM, Guttman M, Huarte M, et al. Many human large intergenic noncoding RNAs associate with chromatin-modifying complexes and affect gene expression. *Proc Natl Acad Sci U S A*. 2009;106(28):11667–11672.
4. Orom UA, Derrien T, Beringer M, et al. Long noncoding RNAs with enhancer-like function in human cells. *Cell*. 2010;143(1):46–58.
5. Rinn JL, Kertesz M, Wang JK, et al. Functional demarcation of active and silent chromatin domains in human HOX loci by noncoding RNAs. *Cell*. 2007;129(7):1311–1323.
6. Calin GA, Liu CG, Ferracin M, et al. Ultraconserved regions encoding ncRNAs are altered in human leukemias and carcinomas. *Cancer Cell*. 2007;12(3):215–229.
7. Ling H, Spizzo R, Atlasi Y, et al. CCAT2, a novel noncoding RNA mapping to 8q24, underlies metastatic progression and chromosomal instability in colon cancer. *Genome Res*. 2013;23(9):1446–1461.
8. Nissan A, Stojadinovic A, Mitrani-Rosenbaum S, et al. Colon cancer associated transcript-1: a novel RNA expressed in malignant and pre-malignant human tissues. *Int J Cancer*. 2012;130(7):1598–1606.
9. Kim T, Cui R, Jeon YJ, et al. Long-range interaction and correlation between MYC enhancer and oncogenic long noncoding RNA CARLo-5. *Proc Natl Acad Sci U S A*. 2014;111(11):4173–4178.
10. Dang CV. MYC on the Path to Cancer. *Cell*. 2012;149(1):22–35.
11. Muzny DM, et al. Comprehensive molecular characterization of human colon and rectal cancer. *Nature*. 2012;487(7407):330–337.
12. Seoane J, Pouponnot C, Staller P, Schader M, Eilers M, Massague J. TGFbeta influences Myc, Miz-1 and Smad to control the CDK inhibitor p15INK4b. *Nat Cell Biol*. 2001;3(4):400–408.
13. Inoue S, Hao Z, Elia AJ, et al. Mule/Huwe1/Arf-BP1 suppresses Ras-driven tumorigenesis by preventing c-Myc/Miz1-mediated down-regulation of p21 and p15. *Genes Dev*. 2013;27(10):1101–1114.
14. Staller P, Peukert K, Kiermaier A, et al. Repression of p15INK4b expression by Myc through association with Miz-1. *Nat Cell Biol*. 2001;3(4):392–399.
15. Oskarsson T, Essers MA, Dubois N, et al. Skin epidermis lacking the c-Myc gene is resistant to Ras-driven tumorigenesis but can reacquire sensitivity upon additional loss of the p21Cip1 gene. *Genes Dev*. 2006;20(15):2024–2029.
16. Rochlitz CF, Herrmann R, de Kant E. Overexpression and amplification of c-myc during progression of human colorectal cancer. *Oncology*. 1996;53(6):448–454.
17. Lee BK, Bhinge AA, Battenhouse A, et al. Cell-type specific and combinatorial usage of diverse transcription factors revealed by genome-wide binding studies in multiple human cells. *Genome Res*. 2011;22(1):9–24.
18. Muppirala UK, Honavar VG, Dobbs D. Predicting RNA-protein interactions using only sequence information. *BMC Bioinformatics*. 2011;12:489.
19. Gao R, Yu Y, Inoue A, Widodo N, Kaul SC, Wadhwa R. Heterogeneous nuclear ribonucleoprotein K (hnRNP-K) promotes tumor metastasis by induction of genes involved in extracellular matrix, cell movement, and angiogenesis. *J Biol Chem*. 2006;288(21):15046–15056.
20. Carpenter B, McKay M, Dundas SR, Lawrie LC, Telfer C, Murray GI. Heterogeneous nuclear ribonucleoprotein K is over expressed, aberrantly localised and is associated with poor prognosis in colorectal cancer. *Br J Cancer*. 2006;95(7):921–927.
21. Wang J, Guo Y, Chu H, Guan Y, Bi J, Wang B. Multiple Functions of the RNA-Binding Protein HuR in Cancer Progression, Treatment Responses and Prognosis. *Int J Mol Sci*. 2013;14(5):10015–10041.
22. Newbold A, Salmon JM, Martin BP, Stanley K, Johnstone RW. The role of p21 and p27 in HDACi-mediated tumor cell death and cell cycle arrest in the Emu-myc model of B-cell lymphoma. *Oncogene*. 2013;33:5415–5423.
23. Zhang J, Lou X, Yang S, et al. BAG2 is a target of the c-Myc gene and is involved in cellular senescence via the p21(CIP1) pathway. *Cancer Lett*. 2011;318(1):34–41.
24. Liu M, Casimiro MC, Wang C, et al. p21CIP1 attenuates Ras- and c-Myc-dependent breast tumor epithelial mesenchymal transition and cancer stem cell-like gene expression in vivo. *Proc Natl Acad Sci U S A*. 2009;106(45):19035–19039.
25. Carnero A, Beach DH. Absence of p21WAF1 cooperates with c-myc in bypassing Ras-induced senescence and enhances oncogenic cooperation. *Oncogene*. 2004;23(35):6006–6011.
26. Takahashi K, Yamanaka S. Induction of pluripotent stem cells from mouse embryonic and adult fibroblast cultures by defined factors. *Cell*. 2006;126(4):663–676.
27. Zheng GX, Do BT, Webster DE, Khavari PA, Chang HY. Dicer-microRNA-Myc circuit promotes transcription of hundreds of long noncoding RNAs. *Nat Struct Mol Biol*. 2014;21(7):585–590.

ARTICLE